

Efficient construction of canonical polyadic approximations of tensor networks

Karl Pierce and Edward F. Valeev*

Department of Chemistry, Virginia Tech, Blacksburg, Virginia 24061, U.S.A.

E-mail: efv@vt.edu

Abstract

We consider the problem of constructing a canonical polyadic (CP) decomposition for a tensor *network*, rather than a single tensor. We illustrate how it is possible to reduce the complexity of constructing an approximate CP representation of the network by leveraging its structure in the course of the CP factor optimization. The utility of this technique is demonstrated for the order-4 Coulomb interaction tensor approximated by 2 order-3 tensors via an approximate generalized square-root (SQ) factorization, such as density fitting or (pivoted) Cholesky. The complexity of constructing a 4-way CP decomposition is reduced from $\mathcal{O}(n^4 R_{\text{CP}})$ (for the non-approximated Coulomb tensor) to $\mathcal{O}(n^3 R_{\text{CP}})$ for the SQ-factorized tensor, where n and R_{CP} are the basis and CP ranks, respectively. This reduces the cost of constructing the CP approximation of 2-body interaction tensors of relevance to accurate many-body electronic structure by up to 2 orders of magnitude for systems with up to 36 atoms studied here. The full 4-way CP approximation of the Coulomb interaction tensor is shown to be more accurate than the known approaches utilizing CP-decomposed SQ factors (also obtained at the $\mathcal{O}(n^3 R_{\text{CP}})$ cost), such as the algebraic pseudospectral and tensor hypercontraction approaches.

The CP decomposed SQ factors can also serve as a robust initial guess for the 4-way CP factors.

1 Introduction

The canonical polyadic (CP) decomposition^{1,2}, also known as CANDECOMP³, PARAFAC⁴, separated representation,⁵ and other names⁶, is a popular data-sparse representation of higher-order tensors as a data analysis tool in many settings as well as a way to reduce the cost and/or complexity of the tensor algebra in some physical simulation applications. The CP decomposition of an order- n tensor can be viewed as a *tensor network* (TN) of n factor matrices, each describing a single mode of the target tensor. What makes the CP TN unique is that each factor matrix is connected directly to *every* other factor via a single *hyperedge*. By treating all modes of the target tensor on equal footing the CP decomposition has a universal structure that simplifies its use compared to other TNs with more specialized topologies (such as matrix product states, etc.). Formally, the CP decomposition reduces the storage complexity of higher-order tensors from exponential to linear in the tensor order. However, finding the minimal extent of the CP hyperedge (CP *rank*) sufficient for exact CP representation of a given tensor or its approximate CP representation to a fixed given precision is hard.^{7,8}

Whether CP decomposition and/or TNs with CP-like hyperedges can be gainfully used in quantum many-body simulation, despite the challenges of computing the CP decomposition, is an open question. Beylkin and Mohlenkamp motivated broad utility of polyadic separation of multidimensional functions and operators (i.e., an infinite-dimensional analog of CP decomposition) and illustrated its effectiveness for model quantum simulation problems.⁵ The only uses of the CP decomposition for *global* approximation of the electronic Hamiltonian and/or wave function have been demonstrated by Auer and co-workers;⁹⁻¹¹ the scope of these applications was limited to small systems by the high cost of the computing and

updating the CP decomposition. More limited uses of the CP decomposition appeared in the context of compressed spectral element representation for constructing numerical (real-space) orbitals by Bischoff and Valeev¹² and for compressing real-space representations of various quantities in the electronic structure context by Chinnamsetty et al.¹³ More common scenario in the quantum many-body simulation is the appearance of tensor networks featuring CP-like hyperedges, e.g., as a result of approximating an integral by a quadrature. Such examples include the approximation of the Coulomb operator in the pseudospectral (PS) family of methods,¹⁴ the related tensor hypercontraction (THC) factorization of 2-particle tensors¹⁵ and its close cousin, interpolative separable density fitting,¹⁶ robust CP-DF factorization marrying the PS and THC approaches,¹⁷ and the CD-SVD compression of the Coulomb interaction tensor¹⁸. These decompositions have productive uses in quantum simulation contexts on both classical¹⁷⁻²¹ and quantum hardware.²² Lastly, the use of Laplace transform in the electronic structure²³ also leads to networks with CP-like hyperedges.

Our recent experiences¹⁷ suggests that more productive uses of the CP factorization can be found when focusing on approximating not *individual* tensors but on tensor *networks*. Thus here we consider a problem of constructing a CP approximation for a tensor network. To the best of our knowledge such class of problems has not been yet considered. It is clear that leveraging the structure of the tensor network in the course of constructing its CP approximation can lead to notable savings. Here we show that that is indeed the case in a practically-important scenario; namely, we show how to construct a full (4-way) CP decomposition of a 2-particle interaction represented in a molecular orbital basis with reduced complexity by leveraging the approximate generalized square root (SQ) factorization of such a tensor. This allows us to construct full CP decomposition of 2-particle interaction tensors for systems of unprecedented size. Such productive combination of CP and other tensor network approximations can be further improved by other CP acceleration strategies such as parallelization²⁴ and improved solver strategies.²⁵⁻²⁷

The rest of the manuscript is organized as follows. Section 2 introduces the mathe-

mathematical formalism for SQ-accelerated CP4 decomposition and its application to the 2-body interaction tensors in quantum electronic structure. Technical details of the computational experiments are described in Section 3. In Section 4 we compared the accuracy of the CP4 decomposition to the more common 3-way CP decompositions as well as illustrate the efficiency of the accelerated CP4 solver relative to its standard (naive) counterpart. Our findings are summarized in Section 5.

2 Formalism

Our objective is to approximate a 2-particle interaction represented in a generic basis $\{\phi_p\}$:

$$g_{st}^{pq} = \iint \phi_s^*(\mathbf{r}_1)\phi_t^*(\mathbf{r}_2)g(\mathbf{r}_1, \mathbf{r}_2)\phi_p(\mathbf{r}_1)\phi_q(\mathbf{r}_2)d\mathbf{r}_1d\mathbf{r}_2; \quad (1)$$

all numerical experiments in this work will use $g(\mathbf{r}_1, \mathbf{r}_2) \equiv |\mathbf{r}_1 - \mathbf{r}_2|^{-1}$ (the Coulomb interaction), but other positive kernels can be used. A CP factorization of g is represented using a set of factor matrices $\mathbf{x} = \{\boldsymbol{\gamma}, \boldsymbol{\rho}, \boldsymbol{\beta}, \boldsymbol{\kappa}\}$:

$$g_{st}^{pq} \stackrel{\text{CP4}}{\approx} \hat{g}_{st}^{pq} = \sum_r^{R_{\text{CP4}}} \lambda_r \gamma_r^p \rho_r^q \beta_s^r \kappa_t^r; \quad (2)$$

moniker ‘‘CP4’’ will be used to help distinguish such 4-way CP factorization from other factorizations involving CP decomposition.

In this work we impose the CP factors be column-wise unit-normalized, i.e. $\sum_p |\gamma_r^p|^2 = 1$, etc. In general, the CP ‘‘singular values’’ λ_r can be absorbed into the factors;¹ the weighted factors will be denoted by a *caron*, $\check{\gamma}_r^p \equiv \lambda_r \gamma_r^p$. Thus, Eq. (2) then can be written equivalently

¹It should be noted that though λ_r s resemble singular values, the CP decomposition does not have the same properties as the singular values decomposition²⁸

using weighted factors:

$$g_{st}^{pq} \stackrel{\text{CP4}}{\approx} \sum_r^{R_{\text{CP4}}} \tilde{\gamma}_r^p \rho_r^q \beta_s^r \kappa_t^r = \sum_r^{R_{\text{CP4}}} \gamma_r^p \tilde{\rho}_r^q \beta_s^r \kappa_t^r = \sum_r^{R_{\text{CP4}}} \gamma_r^p \rho_r^q \tilde{\beta}_s^r \kappa_t^r = \sum_r^{R_{\text{CP4}}} \gamma_r^p \rho_r^q \beta_s^r \tilde{\kappa}_t^r \quad (3)$$

There exists no finite algorithm to determine the exact or approximate (sufficient for a given accuracy) CP rank of a general tensor^{7,8}. Thus in practice the CP rank is determined heuristically. For a fixed CP rank Eq. (2) is typically constructed by minimizing the norm of the error,

$$f(\mathbf{x}) \equiv \frac{1}{2} \sum_{pqst} |g_{st}^{pq} - \hat{g}_{st}^{pq}|^2. \quad (4)$$

The nonlinear optimization uses well-known heuristics (Alternating Least Squares (ALS)^{3,5,29}, accelerated gradient^{9,30-33}, nonlinear least squares³⁴, etc.) whose cost-determining step is the evaluation of the objective function's gradient (or its components):

$$\frac{\partial f}{\partial \tilde{\gamma}_p^r} = 2 \sum_{qst} (\hat{g}_{pq}^{st} - g_{pq}^{st}) \rho_r^q \beta_s^r \kappa_t^r = 2 \left(\sum_{r'} \tilde{\gamma}_p^{r'} (\mathbf{W}^{\{\gamma\}})_{r'}^r - \sum_{qst} g_{pq}^{st} \rho_r^q \beta_s^r \kappa_t^r \right), \quad (5)$$

where

$$(\mathbf{W}^{\{\gamma\}})_{r'}^r \equiv \left(\sum_q \rho_q^{r'} \rho_q^r \right) \left(\sum_s \beta_s^r \beta_s^{r'} \right) \left(\sum_t \kappa_t^r \kappa_t^{r'} \right). \quad (6)$$

The simplest way to update CP factors is via ALS, by (1) solving the linear least squares problem $\partial f / \partial \tilde{\gamma}_p^r = 0$ for $\tilde{\gamma}^2$, (2) normalizing its columns to obtain updated γ and λ , and repeating for other factors until the desired ALS convergence criterion (ϵ_{ALS} has been achieved (here we use the criterion of Ref.¹⁷), and repeating as necessary. Computing the last term in Eq. (5), which is needed both in ALS and in the gradient-based approaches, is the cost-determining step, with a complexity of $\mathcal{O}(N^4 R)$, where N is proportional to the

²Since matrix \mathbf{W} is Hermitian, fast (pivoted) Cholesky solver for the linear system can be used.

mode dimension and R is the CP rank (in practice $R \propto \mathcal{O}(N)$). The high-order cost of the gradient evaluation is aggravated by the difficulty of the optimization problem (strong nonlinearity, sensitivity to the initial guess, and often poor conditioning; e.g., see Ref. 35) These factors explain why the CP4 decomposition has barely been explored in the context of quantum simulation, as mentioned in Section 1.

Popular CP-like approximations of g can be determined by starting from the generalized³ square root (SQ) factorization:

$$g_{st}^{pq} \overset{\text{SQ}}{\approx} \sum_X B_s^{pX} B_t^{qX}. \quad (7)$$

The two most popular ways to determine the square root factor B are the density fitting^{36–39} (DF) approximation, in which X represents a predetermined fitting (“auxiliary”) basis that grows linearly with the system size, and the rank-revealing Cholesky decomposition (CD).^{40–43} The error of Eq. (7) can be controlled in the case of DF by using a more complete fitting basis, or in the case of CD by increasing the Cholesky rank.

Although the generalized square root factorization is extremely popular, due to its ability to reduce the storage complexity of g from N^4 to N^3 , it rarely reduces the computational complexity of electronic structure methods by itself. However, by combining Eq. (7) with the CP decomposition it is possible to reduce the computational complexity for several important algorithms, such as the exact exchange evaluation.^{14,44} Traditionally, this is accomplished by CP factorizing the tensor B :

$$B_s^{pX} \approx \hat{B}_s^{pX} = \sum_r^{R_{\text{CP}3}} \lambda_r \gamma_r^p \beta_s^r \chi_r^X = \sum_r^{R_{\text{CP}3}} \gamma_r^p \beta_s^r \tilde{\chi}_r^X, \quad (8)$$

where $R_{\text{CP}3}$ is the CP rank of this decomposition; we will refer to a 3-way CP decomposition by moniker “CP3”. Note that although Eq. (8) does not impose the hermiticity of B (with

³A square root B of matrix/operator A satisfies $A = BB$. In some contexts, such as Kalman filtering, B such that $A = B^\dagger B$, for positive A , is also referred to as square root. To avoid confusion we will refer to such B as generalized square root of A .

respect to swapping of p and s), in practice $\gamma_r^p = (\beta_p^r)^*$ can be imposed.^{17,45} The CP3 approximation can then be introduced into Eq. (7):

- *once*

$$g_{st}^{pq} \approx \sum_X \hat{B}_s^{pX} B_t^{qX} = \sum_r^{R_{\text{CP3}}} \gamma_r^p \beta_s^r \left(\sum_X \tilde{\chi}_r^X B_t^{qX} \right) \equiv \sum_r^{R_{\text{CP3}}} \gamma_r^p \beta_s^r \tilde{B}_{qr}^t, \quad (9)$$

to produce a factorization of the pseudospectral (PS) method^{14,46–54};

- *twice*,

$$g_{st}^{pq} \approx \sum_X \hat{B}_s^{pX} \hat{B}_t^{qX} = \sum_{r,r'}^{R_{\text{CP3}}} \gamma_r^p \beta_s^r \gamma_{r'}^q \beta_t^{r'} \left(\sum_X \tilde{\chi}_r^X \tilde{\chi}_{r'}^X \right) \equiv \sum_{r,r'}^{R_{\text{CP3}}} \gamma_r^p \beta_s^r \gamma_{r'}^q \beta_t^{r'} \tilde{\chi}_{r,r'}, \quad (10)$$

to produce the tensor hypercontraction format^{15,20,44,45,55–60}; or

- *robustly*¹⁷ using a combination of single and double substitutions,

$$g_{st}^{pq} \approx \sum_X \hat{B}_s^{pX} B_t^{qX} + \sum_X B_s^{pX} \hat{B}_t^{qX} - \sum_X \hat{B}_s^{pX} \hat{B}_t^{qX}. \quad (11)$$

The latter, denoted as rCP3-DF, has been shown recently¹⁷ to be more accurate than either Eq. (9) or Eq. (10). As we demonstrate next, the “square-root” factorization can be also useful as a *precursor* to the CP4 approximation of g . Specifically, its use allows one to reduce the complexity of constructing the CP4 approximation from $\mathcal{O}(N^5)$ to $\mathcal{O}(N^4)$.

As mentioned above, evaluation of the gradient of the CP objective function, Eq. (5), costs $\mathcal{O}(N^4 R)$. However, it is possible to reduce the complexity of the CP optimization problem by replacing tensor g with its SQ-factorization, Eq. (7):

$$\begin{aligned} \frac{\partial f}{\partial \tilde{\gamma}_p^r} &\stackrel{\text{SQ}}{=} 2 \sum_{qst} \left(\hat{g}_{pq}^{st} - \sum_X \sum_X B_{pX}^s B_{qX}^t \right) \rho_r^q \beta_s^r \kappa_t^r \\ &= 2 \left(\sum_{r'} \tilde{\gamma}_p^{r'} (\mathbf{W}^{\{\gamma\}})_{r'}^r - \sum_X (B_{pX}^s \beta_s^r) \left(\sum_{qt} B_{qX}^t \rho_r^q \kappa_t^r \right) \right). \end{aligned} \quad (12)$$

Using the SQ-network approximated CP4 loss function, we reduce the cost of the gradient of CP4 from $\mathcal{O}(N^4R)$ to $\mathcal{O}(N^2RX)$. Furthermore, we reduce the storage requirements of the approach from $\mathcal{O}(N^4 \approx N^3R)$ to $\mathcal{O}(N^3 \approx N^2R)$. Although others have introduced TNs into the CP loss function⁵⁹, this work is first to construct factor matrices for *only* the external modes of a TN. The CP decomposition, in this way, provides a route to approximate the result of a TN without *a priori* construction of the tensor from the network. Clearly, such use of CP can be more generally useful than just for the case of the Coulomb integrals.

Now, formally the CP4 ALS optimization has the same computation scaling as the CP3 ALS optimization, $\mathcal{O}(N^4)$. However, it is known that the efficiency of the CP optimization process and the accuracy of the resulting factorization can strongly depend on an initial guess. In this work we utilize an initial guess scheme which uses the CP3-SQ-factorization of g as well as vectors filled with quasi-random numbers taken from a uniform distribution on $[-1,1]$. To motivate our initialization strategy, we compare the CP4-approximated g to its THC-like CP3-SQ counterpart:

$$g_{st}^{pq} \stackrel{\text{Eq. (2)}}{\approx} \sum_r^{R_{\text{CP4}}} \gamma_r^p \beta_s^r \rho_r^q \kappa_t^r \lambda_r \quad (13)$$

$$g_{st}^{pq} \stackrel{\text{Eq. (10)}}{\approx} \sum_{r,r'}^{R_{\text{CP3}}} \gamma_r^p \beta_s^r \gamma_{r'}^q \beta_{t'}^{r'} \tilde{\chi}_{r,r'} \quad (14)$$

The key differences between these expressions are: (1) factors γ and β in Eqs. (13) and (14) were determined to CP-approximate different tensors (g_{st}^{pq} and B_s^{pX} , respectively), and (2) Eq. (14) is explicitly particle-symmetric. Importantly, however, the CP3-SQ approximation (Eq. (14)) can be rewritten in the CP4 form *exactly* by merging indices into a composite index $w \equiv \{r, r'\}$:

$$g_{st}^{pq} \stackrel{\text{Eq. (14)}}{\approx} \sum_w^{R_{\text{CP3}}^2} \gamma_w^p \beta_s^w \rho_w^q \kappa_t^w \lambda_w \quad (15)$$

where

$$\gamma_w^p \equiv \gamma_{\{r,r'\}}^p \equiv \gamma_r^p \otimes \mathbb{I}_{r'}, \quad (16)$$

$$\beta_s^w \equiv \beta_s^{\{r,r'\}} \equiv \beta_s^r \otimes \mathbb{I}_{r'}, \quad (17)$$

$$\rho_w^q \equiv \rho_{\{r,r'\}}^q \equiv \gamma_{r'}^q \otimes \mathbb{I}_r, \quad (18)$$

$$\kappa_t^w \equiv \kappa_t^{\{r,r'\}} \equiv \beta_t^{r'} \otimes \mathbb{I}_r. \quad (19)$$

$$\lambda_w \equiv \tilde{\chi}_{r,r'} \quad (20)$$

such that \otimes represents the outer product and \mathbb{I}_r is an identity vector with dimension r . In practical applications of THC the CP3 rank is $\mathcal{O}(N)$, thus it may appear that the CP4 rank required to represent it exactly is $\mathcal{O}(N^2)$. However since FMM⁶¹ and related approximations⁶² can be used to construct representations of sufficiently-well-behaved integral operators with $\mathcal{O}(N \log N)$ complexity, this limits the asymptotic CP4 rank of g to $\mathcal{O}(N \log N)$ as well. In the context of THC, this asymptotic limit means that the $\tilde{\chi}$ matrix can be made sparse for sufficiently large systems by an appropriate transformation. However, for small systems where the $\tilde{\chi}$ matrix is dense, direct construction of CP4 can be more compact than the THC representation, i.e. a CP4 approximation with an accuracy of ϵ_{THC} can be found via an optimization of a rank $R_{\text{CP4}} \ll R_{\text{CP3}}^2$ CP4-ALS decomposition (see Section 4 for details).

The formal connection between Eq. (2) and Eq. (14) via Eq. (15) thus suggests the use of unit-normalized CP3 factors as the initial guess for the CP4 decomposition. Further, because the CP optimization recomputes λ every iteration, it is not necessary to keep elements of the diagonalized $\tilde{\chi}$ matrix (in Eq. (14)). If the target CP4 rank is greater than the CP3 rank, the CP4 factors can be padded with vectors of quasi-random numbers taken from the uniform distribution on $[-1,1]$ and normalized to unity. This is sufficient to bootstrap the ALS CP4 solver since, again, the singular values are not needed to compute the gradient with respect to the weighted factors (see Eq. (5)).

3 Computational details

The CP3 and CP4 optimization computations have been computed using the Basic Tensor Algebra Subroutine (BTAS) software package⁶³. All of these computations were run on the Virginia Tech Advanced Research Computing’s (ARC) Cascades cluster which utilizes standard nodes that contain 2 Intel Xeon E5-2683 v4 CPUs. The CP approximations were computed using the standard alternating least squares (ALS) method.^{5,64} In this work, as was done in our previous work,¹⁷ initial CP3 factors were generated using quasi-random numbers taken from the uniform distribution on [-1,1]. As discussed earlier in this work, we utilized both optimized CP3 factors and quasi-random numbers as an initial guess strategy for the CP4 decomposition.

Assessment of the CP factorizations utilized the a small subset of 5 complexes from the S66 (S66/5) benchmark set of weakly-bound complexes⁶⁵⁴. The S66 geometries were taken from the Benchmark Energy and Geometry Database (BEGDB).⁶⁶ Additionally, the a conformer of $(\text{H}_2\text{O})_{12}$ ^{67,68} is used to demonstrate the capacity of the reduced-scaling CP4 ALS optimization strategy. All of the above computations utilized the aug-cc-pVDZ^{69,70} (aVDZ) orbital basis set (OBS). The 2-electron interaction tensors were approximated using standard Coulomb-metric density fitting using the aug-cc-pVDZ-RI (abbreviated as aVDZ-RI) density fitting basis set (DFBS).⁷¹ Assessment of the basis set variation in the performance of CP4 used the following additional OBS/DFBS pairs: the cc-pVDZ-F12 (abbreviated as DZ-F12)⁷² OBS paired with the aVDZ-RI DFBS, the aug-cc-pVTZ (aVTZ) OBS^{69,70} paired with the aug-cc-pVTZ-RI⁷¹ (aVTZ-RI) DFBS, and the cc-pVTZ-F12⁷² (TZ-F12) OBS paired with the aVTZ-RI DFBS.

Lastly, to make comparisons between different systems the CP ranks will be defined in units of size X of the DF fitting (“auxiliary”) basis, which grows proportionally to the number of atoms in the system.

⁴1 water ... water, 2 water ... MeOH, 3 water ... MeNH₂, 4 MeNH₂ ... MeOH, 5 ethyne ... water (CH-O)

4 Results

Figures 1 and 2 illustrate the accuracy of the CP4 approximation compared to CP3-DF-based approximations. To compare tensor network approximations to each other it is necessary to map all of them to a common network topology, i.e., the CP3-DF tensor networks are mapped their CP4 counterpart via Eq. (15). Since a CP3-DF network with rank R_{CP3} is represented exactly by a CP4 network with rank $R_{\text{CP4}} = R_{\text{CP3}}^2$ (see the discussion around Eq. (15)), the CP4 network of rank R_{CP4} are compared to the CP3 counterparts of rank $R_{\text{CP3}} = \sqrt{R_{\text{CP4}}}$. Furthermore, since the robust CP3-DF approximant (Eq. (11)) is a sum of 3 contributions it makes sense to use even an lower CP3 rank ($\sim \sqrt{R_{\text{CP4}}/3}$) when comparing to a CP4 network. For the sake of simplicity, we conservatively use the same CP3 rank for all CP3-based networks.

In Figures 1 and 2 the {dashed, solid} lines denoted ‘‘DF’’ show the {maximum, average} elementwise errors due to the DF approximation of the exact g tensors, while the other lines show the corresponding elementwise errors associated with the CP decomposition of the DF-approximated g tensors. The lines labeled ‘‘CP3’’ correspond to the THC-like CP3-DF approximation of the g tensors (Eq. (14)) and the lines labeled ‘‘rCP3’’ correspond to the robust CP3-DF approximation (Eq. (11)). The lines labeled ‘‘CP4’’ correspond to the CP4 decomposition using the DF-approximated g tensor in the CP4 ALS optimization. Finally, the lines labeled ‘‘Optimal CP3’’ correspond to the CP3-DF approximation (Eq. (14)) in which the constituent factors were optimized to make stationary an *augmented* CP loss function defined for, e.g., g_{ci}^{ab} as

$$f(\mathbf{x}_1, \mathbf{x}_2) = \frac{1}{2} \|B_c^{aX} B_i^{bX} - \hat{B}_c^{aX} \hat{B}_i^{bX}\|^2 + \frac{1}{2} \|B_c^{aX} - \hat{B}_c^{aX}\|^2 + \frac{1}{2} \|B_i^{bX} - \hat{B}_i^{bX}\|^2, \quad (21)$$

where $\mathbf{x}_{\{1,2\}}$ are the CP3 parameters defining $\{\hat{B}_c^{aX}, \hat{B}_i^{bX}\}$. The augmented CP loss function is designed to simultaneously solve 3 *coupled* least-squares problems, namely (1) finding

the optimal CP3 factors for approximating the (DF-approximated) g_{ci}^{ab} using the CP3-DF network, (2,3) finding the optimal CP3 factors for approximating the $\{B_c^{aX}, B_i^{bX}\}$ DF factors, respectively. Coupling the three CP problems helps the ALS solver to avoid excessively large steps that may occur when solving problem 1 alone, which stems from lack of convergence guarantees for the ALS algorithm in general.²⁸ Similar modifications of the objective functions to penalize large steps have been used by others.²² The use of more robust direct minimization solvers for the CP and general tensor network optimization problems (e.g., nonlinear quasi-Newton solvers with step restriction) should alleviate the need for augmenting the CP3-DF objective function.

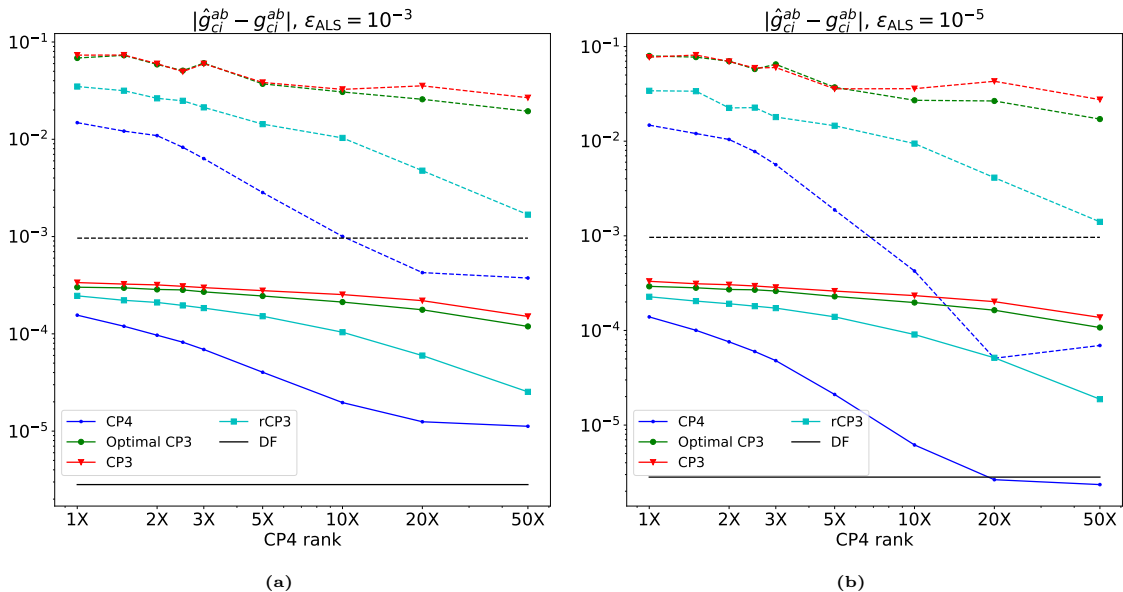


Figure 1: Absolute average element error for approximated g_{ci}^{ab} tensor using an ALS solver threshold¹⁷ of (a) $\epsilon_{\text{ALS}} = 10^{-3}$ and (b) $\epsilon_{\text{ALS}} = 10^{-5}$. Solid lines represent mean error and dashed lines represent max error. Note that the CP4 rank is in units of a factor times the DF fitting basis, a metric which grows linearly with rank. Data was collected using the S66/5 dataset with a aVDZ/aVDZ-RI basis

As Figures 1 and 2 clearly demonstrate, at equivalent ranks the CP4 approximation is more accurate than the CP3-DF counterparts. CP4 even surpasses the accuracy of the robust CP3-DF variant which we recently showed to be more accurate than the corresponding PS-like and THC-like CP3-DF counterparts. Namely, CP4 is always more accurate than rCP3-DF for the g_{ci}^{ab} tensor and surpasses accuracy of the latter with largest CP4 rank for the g_{cd}^{ab} tensor. However, notice that at modest ranks the accuracy of the CP4 approximation

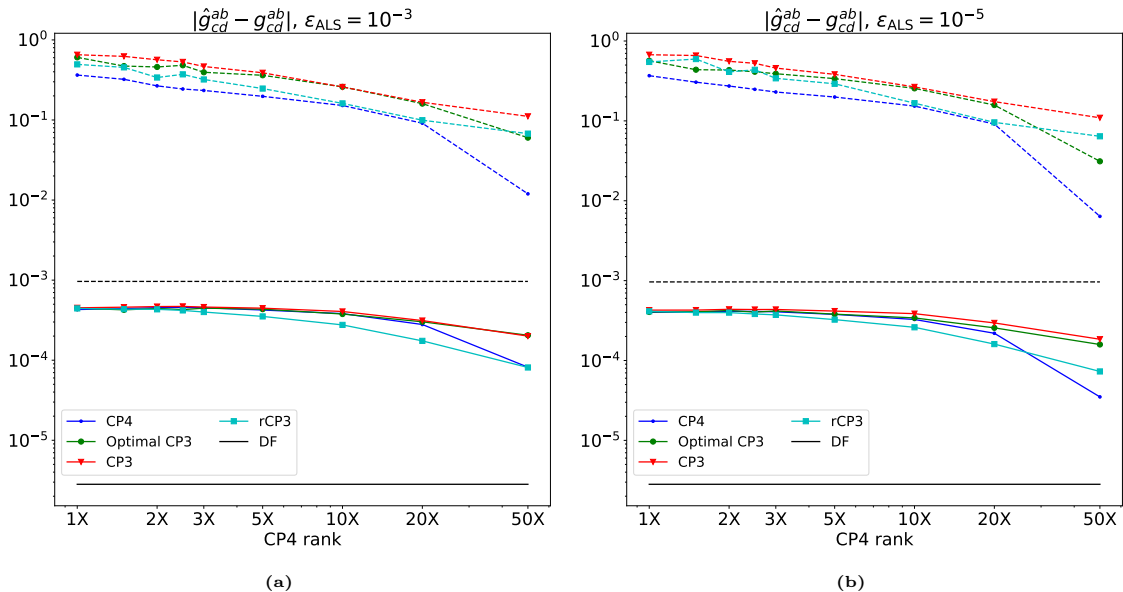


Figure 2: Absolute average element error for approximated g_{cd}^{ab} tensor using an ALS solver threshold¹⁷ of (a) $\epsilon_{ALS} = 10^{-3}$ and (b) $\epsilon_{ALS} = 10^{-5}$. Solid lines represents mean error and dashed lines represent max error. Note that the CP4 rank is in units of a factor times the DF fitting basis, a metric which grows linearly with rank. Data was collected using the S66/5 dataset with a aVDZ/aVDZ-RI basis

of g_{cd}^{ab} was found to be lower than that of the robust CP3 approximation, see the solid lines in Figure 2. As discussed above, this is likely due to the overly conservative choice of the relationship between the CP3 and CP4 ranks for the robust case (i.e. the rank for the rCP3 approximation should have been smaller by a factor of $\sqrt{3}$).

CP4 errors usually, but not always, decrease monotonically: for example, the average CP4 error for g_{ci}^{ab} (Figure 1a) does not decrease substantially when the CP rank is increased from $20X$ to $50X$. This can be rationalized if we recall that the error of an approximate CP4 decomposition is due to 2 factors: finiteness of the CP4 rank (hence controlled by the rank) and the suboptimality of the factors (controlled by the ALS convergence threshold ϵ_{ALS}). As the CP4 rank increases the factor optimization error becomes dominant. Indeed, as the ALS threshold decreases from the 10^{-3} to 10^{-5} this artifact disappears as well as the total errors for large ranks ($\geq 5X$) decrease significantly. This result is consistent with our previous finding for the CP3 optimization.¹⁷ It is well understood that more robust CP solvers^{25,73-75} can be employed to improve the convergence rate related issues. Since our focus here is primarily on addressing the universal concerns (the cost of gradient evaluation,

initial guess) that apply to all CP solvers, here we only use ALS and postpone the use of improved CP solvers to later studies.

Another important phenomenon becomes apparent when we plot the distribution of tensor element magnitudes for the two types of tensors in the two test systems (Figure 3). One of the two test systems (namely, the water dimer) has geometrical symmetry that makes many tensor elements nearly zero; note that our orbital solver does not exploit geometrical symmetry and therefore the zeroes are *soft* (i.e., the elements that are zero by symmetry are merely small). The presence of symmetry results in markedly bimodal distributions of the element magnitudes for both types of tensors for the water dimer (Figures 3a and 3c), with the “left” peak corresponds to the elements of the exact tensor that are nearly zero by symmetry. However, the distribution of the elements in the CP-approximated tensors are unimodal, except for the highest-rank approximants to the g_{ci}^{ab} tensor. As the CP4 rank increases the largest tensor elements get approximated better and better, whereas the near-zero elements are not well-approximated (in relative sense) even with the largest CP4 ranks employed here. The inability to preserve the blocked structure of the tensor is due to the global character of the CP4 factorization; to impose a blocked structure on the CP approximant would sacrifice the simplicity of the ansatz, hence was not done here.

Besides the block-sparse structure of the tensor approximate CP decomposition also fails to preserve permutational symmetries of the tensor. For example, consider permutational symmetry of the (real) g_{cd}^{ab} tensor:

$$g_{cd}^{ab} = g_{cb}^{ad} = g_{ad}^{cb} = g_{ab}^{cd} = g_{dc}^{ba} = g_{da}^{bc} = g_{bc}^{da} = g_{ba}^{dc}. \quad (22)$$

The CP4 approximant \hat{g}_{cd}^{ab} (Eq. (2)) in general (i.e., for an arbitrary choice of CP4 parameters) lacks the symmetries of the exact tensor. Since it is possible in general to represent g_{cd}^{ab} exactly in the CP4 form, the CP4 factors must have particular structure for the approximant to possess the exact symmetries of the tensor. Hence we inspected the magnitude of the

deviation of the CP4-approximated g_{cd}^{ab} tensors from the exact 8-fold symmetry in Eq. (22) as a function of the CP4 rank. Table Section 4 illustrates how the error of the standard non-symmetrized CP4 approximant compares to that of a (posteriori) symmetrized CP4

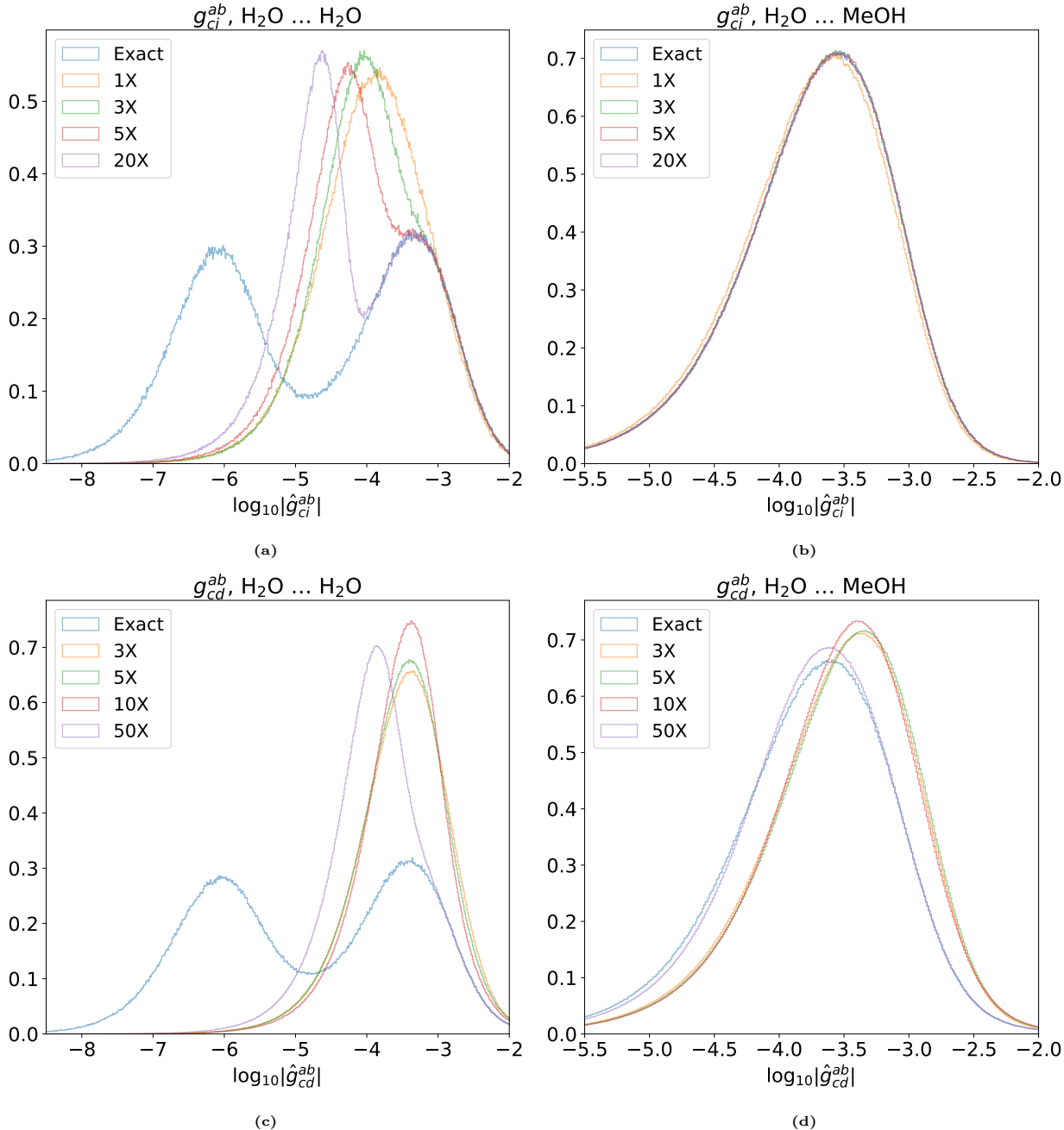


Figure 3: Distributions of the absolute element values for g_{ci}^{ab} [subfigures (a) and (b)] and g_{cd}^{ab} [subfigures (c) and (d)] tensors for representative systems. “Exact” refers to the DF-based tensor free of CP approximations, while “nX” corresponds to the counterpart approximated with CP4 decomposition of rank nX . All computations utilized a aVDZ/aVDZ-RI basis and $\epsilon_{\text{ALS}} = 10^{-3}$.

approximant,

$$\hat{S}\hat{g}_{cd}^{ab} \equiv \frac{1}{8} (\hat{g}_{cd}^{ab} + \hat{g}_{cb}^{ad} + \hat{g}_{ad}^{cb} + \hat{g}_{ab}^{cd} + \hat{g}_{dc}^{ba} + \hat{g}_{da}^{bc} + \hat{g}_{bc}^{da} + \hat{g}_{ba}^{dc}). \quad (23)$$

There are several conclusion that can be drawn from this data. First, the violation of the exact symmetries is relatively small compared to the error due to the error of the CP4 approximant, ranging from $\sim 1\%$ with $R_{\text{CP4}} = X$ to $\sim 30\%$ with $R_{\text{CP4}} = 50X$. Second, enforcing the symmetry always reduces the error. Since for some applications it may be worthwhile to enforce the symmetry by construction it would be potentially useful in the future to explore symmetry-adapted CP ansatze.

Table 1: Comparison of standard (Eq. (2)) and symmetrized (Eq. (23)) CP4 approximants to DF-approximated g_{cd}^{ab} evaluated with the aVDZ/aVDZ-RI basis set pair; the corresponding error 2-norms are denoted by $\|g - \hat{g}\|$ and $\|g - \hat{g}_{\text{sym}}\|$, respectively. $\|\hat{g} - \hat{g}_{\text{sym}}\|$ denotes the 2-norm of the difference between the standard and symmetrized CP4 approximants.

System	Measure	R_{CP4}/X									
		1	1.5	2	2.5	3	5	10	20	50	
(H ₂ O) ₂	$\ g - \hat{g}\ $	17.0	16.1	15.3	14.6	13.9	11.6	8.01	3.15	0.854	
	$\ g - \hat{g}_{\text{sym}}\ $	16.9	15.8	14.9	14.2	13.5	11.2	7.61	2.63	0.612	
	$\ \hat{g} - \hat{g}_{\text{sym}}\ $	2.34	2.96	3.38	3.45	3.29	2.77	2.52	1.74	0.595	
H ₂ O ... MeOH	$\ g - \hat{g}\ $	23.1	22.1	21.3	20.5	19.9	17.6	13.9	8.71	1.05	
	$\ g - \hat{g}_{\text{sym}}\ $	22.9	21.8	20.9	20.1	19.4	17.1	13.3	8.01	0.763	
	$\ \hat{g} - \hat{g}_{\text{sym}}\ $	3.31	3.60	4.01	4.13	4.12	3.84	3.88	3.41	0.718	

Figure 4 illustrates the wall time per ALS iteration with and without the DF approximation of the the CP4 gradient (Eq. (12)) as well as the corresponding speedup (i.e., reduction in computational time per ALS iteration), versus the CP4 rank for the molecules in the S66/5 dataset. With the aVDZ/aVDZ-RI basis set pair the average observed reduction in per-iteration cost is ~ 30 . The speedup figure is clearly basis-dependent, as illustrated using 4 different OBSs for the water dimer in Figure 5; speedups as large as 100 have been observed.

Finally, we use the DF-accelerated CP4 ALS optimization to decompose the g_{ci}^{ab} tensor for a (H₂O)₁₂ cluster in the aVDZ/aVDZ-RI basis and report the results in Section 4. The size of this tensor is 31 GB, which is two orders of magnitude larger than the largest tensors that

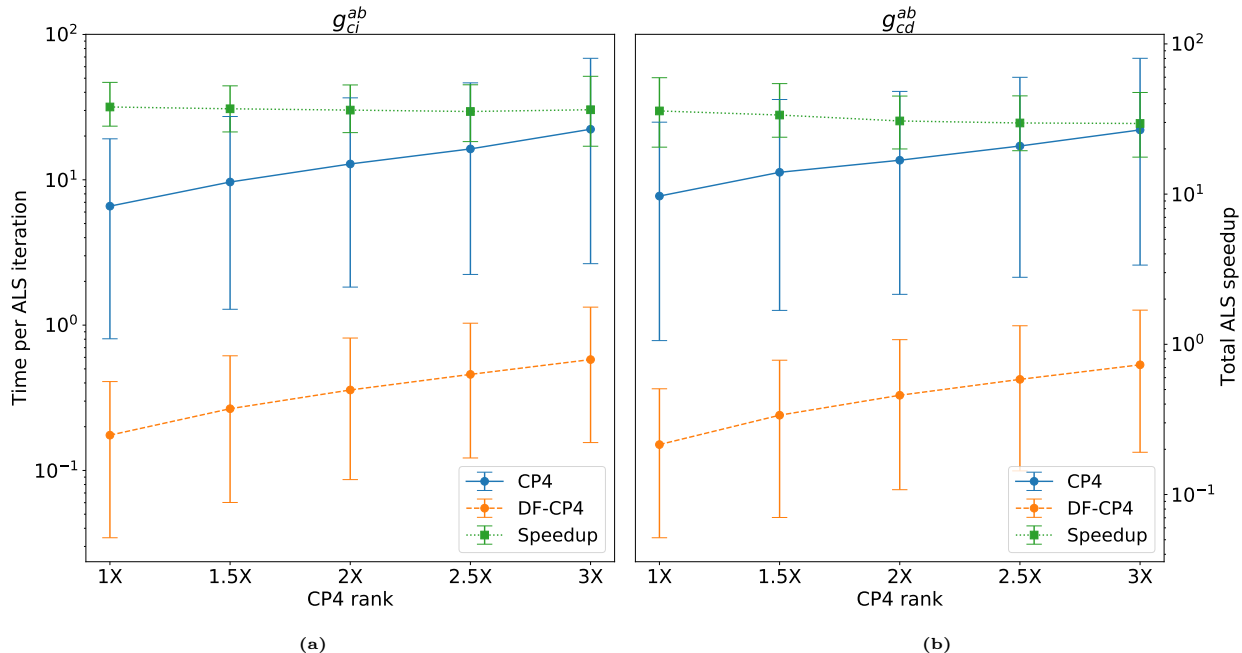


Figure 4: The cost per iteration of the exact and DF approximated CP4 ALS decomposition and the total speedup associated with the DF approximation, i.e. $\frac{t_{\text{exact}}}{t_{\text{DF}}}$. The error bars represent the maximum and minimum per iteration cost. Data was collected using the S66/5 dataset and the aVDZ/aVDZ-RI basis pair.

have previously been decomposed using CP4 in the chemistry context.⁹ Not only are we able to construct a CP4 decomposition of this high-cost integral tensor, but we can systematically improve the accuracy by increasing rank while maintaining a relatively small number of ALS iterations and thus low computational cost.

Table 2: Computation of the CP4 decomposition of the g_{ci}^{ab} tensor for a $(\text{H}_2\text{O})_{12}$ cluster using DF approximated CP4 ALS optimization strategy and using CP3 factor matrices as an initial guess using $R_{\text{CP3}} = R_{\text{CP4}}$. The CP3 iteration’s column shows the number of iterations required to compute the CP3 decomposition of B_c^{aX}/B_{iX}^c . The CP4 time reported does not include the time it takes to construct the CP3 initial guess because there is no one best, unique way to construct the guess. The max and mean error are the element-wise error $|g_{ci}^{ab} - \hat{g}_{ci}^{ab}|$

CP4 Rank	1.0	1.5	2.0	2.5	3.0
CP3 iterations	10/8	10/8	9/9	9/10	8/11
CP4 iterations	21	21	22	24	24
Per iteration cost (s)	9.62	15.5	22.6	30.8	29.8
CP4 time (s)	202	325	498	739	716
Max error	8.05×10^{-3}	7.72×10^{-3}	6.71×10^{-3}	6.17×10^{-3}	5.92×10^{-3}
mean error	2.48×10^{-5}	2.06×10^{-5}	1.82×10^{-5}	1.62×10^{-5}	1.49×10^{-5}

5 Summary and Perspective

We demonstrated how to efficiently compute full (4-way) CP decomposition of large 2-body interaction tensors of relevance to electronic structure simulations by (1) reducing the cost

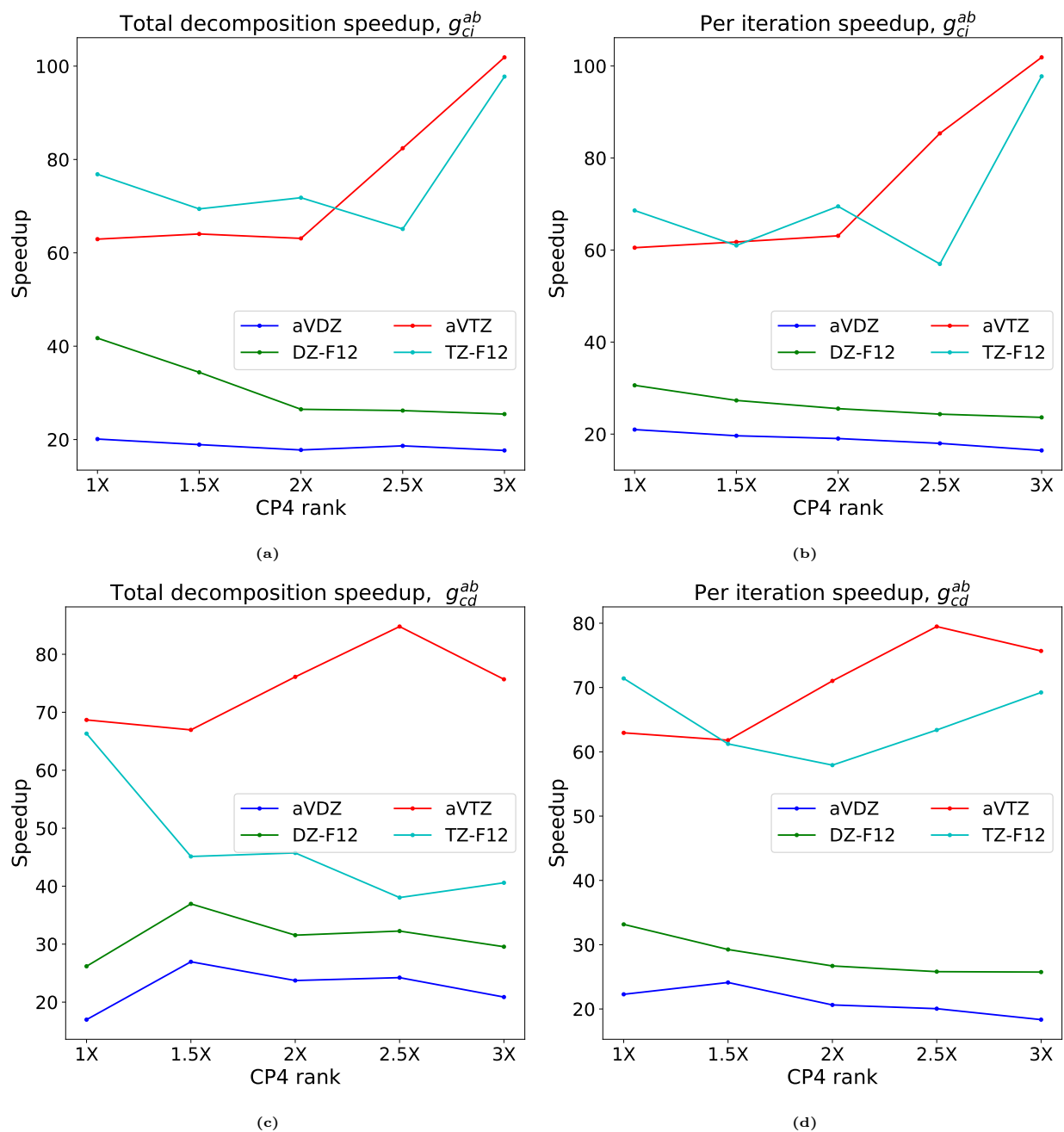


Figure 5: The total speedup of the CP4 ALS optimization of the (a) g_{ci}^{ab} tensor and (c) g_{cd}^{ab} tensor and the per iteration speedup of the (b) g_{ci}^{ab} tensor and (d) g_{cd}^{ab} tensor using a $(\text{H}_2\text{O})_2$ cluster from the S66 dataset and 4 different orbital and DF basis sets

of the CP gradient evaluation via a generalized square root (SQ) decomposition (such as density fitting or Cholesky decomposition), and (2) using 3-way CP decomposition of the SQ factors to construct initial guess for the 4-way CP decomposition. These improvements permit us to compute CP decompositions with greater speed and lower storage requirements than previously possible. 4-way CP decomposition of Coulomb integral tensors with 3 and 4 virtual indices was demonstrated to be more compact and/or accurate than the corresponding combinations of 3-way CP decompositions (similar to the pseudospectral and THC approximations) for several small clusters in the standard S66 benchmark set; practicality of a DF-accelerated 4-way CP solver was demonstrated for the 3-virtual-index integral tensor of a system with 36 atoms.

The techniques described in this paper are more generally applicable than just for approximating the 2-body interaction tensors in the electronic structure domain. The key lesson here is that it can be much more efficient to compute a CP approximation of a target tensor using a representative tensor network in place of the (reconstructed or exact) tensor itself. This suggests that the CP factorization, which offers the most complete decoupling of the tensor modes compared to other tensor network topology, may be more broadly deployable than currently thought, by combining it with other tensor network approximations. We will demonstrate productive uses of CP4 approximation in the context of correlated electronic structure models elsewhere soon.

Acknowledgement

This work was supported by the U.S. Department of Energy award DE-SC0022263 provided via the Scientific Discovery through Advanced Computing (SciDAC) program by the Offices of Advanced Scientific Computing Research (ASCR) and Basic Energy Sciences (BES). We also acknowledge Advanced Research Computing at Virginia Tech (www.arc.vt.edu) for providing computational resources and technical support that have contributed to the results

reported within this paper.

References

- (1) Hitchcock, F. L. The Expression of a Tensor or a Polyadic as a Sum of Products. *J. Math. Phys.* **1927**, *6*, 164–189.
- (2) Kiers, H. A. L. Towards a Standardized Notation and Terminology in Multiway Analysis. *J. Chemometrics* **2000**, *14*, 105–122.
- (3) Carroll, J. D.; Chang, J.-J. Analysis of Individual Differences in Multidimensional Scaling via an N-Way Generalization of “Eckart-Young” Decomposition. *Psychometrika* **1970**, *35*, 283–319.
- (4) Harshman, R. A. Foundations of the PARAFAC Procedure: Models and Conditions for an “Explanatory” Multimodal Factor Analysis. *UCLA Work. Pap. Phon.* **1970**, *16*, 1–84.
- (5) Beylkin, G.; Mohlenkamp, M. J. Numerical Operator Calculus in Higher Dimensions. *Proc. Natl. Acad. Sci.* **2002**, *99*, 10246–10251.
- (6) Möcks, J. Topographic Components Model for Event-Related Potentials and Some Biophysical Considerations. *IEEE Trans. Biomed. Eng.* **1988**, *35*, 482–484.
- (7) Hastad, J. Tensor rank is NP-complete. *Algorithms* **1990**, *11*, 644–654.
- (8) Hillar, C. J.; Lim, L.-H. Most Tensor Problems Are NP-Hard. *J. ACM* **2013**, *60*, 1–39.
- (9) Benedikt, U.; Auer, A. A.; Espig, M.; Hackbusch, W. Tensor Decomposition in Post-Hartree–Fock Methods. I. Two-electron Integrals and MP2. *J. Chem. Phys.* **2011**, *134*, 054118.

- (10) Benedikt, U.; Bohm, K.-H.; Auer, A. A. Tensor decomposition in post-Hartree–Fock methods. II. CCD implementation. *J. Chem. Phys.* **2013**, *139*, 224101.
- (11) Böhm, K. H.; Auer, A. A.; Espig, M. Tensor representation techniques for full configuration interaction: A Fock space approach using the canonical product format. *J. Chem. Phys.* **2016**, *144*, 244102.
- (12) Bischoff, F. A.; Valeev, E. F. Low-Order Tensor Approximations for Electronic Wave Functions: Hartree-Fock Method with Guaranteed Precision. *J. Chem. Phys.* **2011**, *134*, 104104.
- (13) Chinnamsetty, S. R.; Espig, M.; Khoromskij, B. N.; Hackbusch, W.; Flad, H.-J. Tensor Product Approximation with Optimal Rank in Quantum Chemistry. *J. Chem. Phys.* **2007**, *127*, 084110.
- (14) Friesner, R. A. Solution of Self-Consistent Field Electronic Structure Equations by a Pseudospectral Method. *Chem. Phys. Lett.* **1985**, *116*, 39–43.
- (15) Hohenstein, E. G.; Parrish, R. M.; Martínez, T. J. Tensor Hypercontraction Density Fitting. I. Quartic Scaling Second- and Third-Order Møller-Plesset Perturbation Theory. *J. Chem. Phys.* **2012**, *137*, 044103.
- (16) Lu, J.; Ying, L. Compression of the Electron Repulsion Integral Tensor in Tensor Hypercontraction Format with Cubic Scaling Cost. *J. Comp. Phys.* **2015**, *302*, 329–335.
- (17) Pierce, K.; Rishi, V.; Valeev, E. F. Robust Approximation of Tensor Networks: Application to Grid-Free Tensor Factorization of the Coulomb Interaction. *J. Chem. Theory Comput.* **2021**, *17*, 2217–2230.
- (18) Peng, B.; Kowalski, K. Highly Efficient and Scalable Compound Decomposition of Two-Electron Integral Tensor and Its Application in Coupled Cluster Calculations. *J. Chem. Theory Comput.* **2017**, *13*, 4179–4192.

- (19) Neese, F.; Wennmohs, F.; Hansen, A.; Becker, U. Efficient, Approximate and Parallel Hartree–Fock and Hybrid DFT Calculations. A ‘chain-of-Spheres’ Algorithm for the Hartree–Fock Exchange. *Chem. Phys.* **2009**, *356*, 98–109.
- (20) Parrish, R. M.; Sherrill, C. D.; Hohenstein, E. G.; Kokkila, S. I. L.; Martínez, T. J. Communication: Acceleration of Coupled Cluster Singles and Doubles via Orbital-Weighted Least-Squares Tensor Hypercontraction. *J. Chem. Phys.* **2014**, *140*, 181102.
- (21) Hu, W.; Lin, L.; Yang, C. Interpolative Separable Density Fitting Decomposition for Accelerating Hybrid Density Functional Calculations with Applications to Defects in Silicon. *J. Chem. Theory Comput.* **2017**, *13*, 5420–5431.
- (22) Goings, J. J.; White, A.; Lee, J.; Tautermann, C. S.; Degroote, M.; Gidney, C.; Shiozaki, T.; Babbush, R.; Rubin, N. C. Reliably Assessing the Electronic Structure of Cytochrome P450 on Today’s Classical Computers and Tomorrow’s Quantum Computers. *Proc. Natl. Acad. Sci. U.S.A.* **2022**, *119*, e2203533119.
- (23) Almlof, J. Elimination of Energy Denominators in Møller—Plesset Perturbation Theory by a Laplace Transform Approach. *Chem. Phys. Lett.* **1991**, *181*, 319–320.
- (24) Karlsson, L.; Kressner, D.; Uschmajew, A. Parallel Algorithms for Tensor Completion in the CP Format. *Parallel Computing* **2016**, *57*, 222–234.
- (25) Acar, E.; Dunlavy, D. M.; Kolda, T. G. A Scalable Optimization Approach for Fitting Canonical Tensor Decompositions. *J. Chemometrics* **2011**, *25*, 67–86.
- (26) Battaglino, C.; Ballard, G.; Kolda, T. G. A Practical Randomized CP Tensor Decomposition. *SIAM J. Matrix Anal. & Appl.* **2018**, *39*, 876–901.
- (27) Ma, L.; Solomonik, E. Accelerating Alternating Least Squares for Tensor Decomposition by Pairwise Perturbation. *Numerical Linear Algebra App* **2022**, *29*.

- (28) Kolda, T. G.; Bader, B. W. Tensor Decompositions and Applications. *SIAM Rev.* **2009**, *51*, 455–500.
- (29) Harshman, R. a. Foundations of the PARAFAC procedure: Models and conditions for an explanatory multimodal factor analysis. *WPP* **1970**, *16*, 1– 84.
- (30) Acar, E.; Dunlavy, D. M.; Kolda, T. G. A scalable optimization approach for fitting canonical tensor decompositions. *J. Chemom.* **2011**, *25*, 67–86.
- (31) Phan, A.-H.; Tichavský, P.; Cichocki, A. Low Complexity Damped Gauss–Newton Algorithms for CANDECOMP/PARAFAC. *SIAM J. Matrix Anal. Appl.* **2013**, *34*, 126–147.
- (32) Tichavsky, P.; Phan, A. H.; Cichocki, A. A further improvement of a fast damped Gauss-Newton algorithm for candecomp-parafac tensor decomposition. 2013 IEEE Int. Conf. Acoust. Speech Signal Process. 2013; pp 5964–5968.
- (33) Espig, M.; Hackbusch, W.; Rohwedder, T.; Schneider, R. Variational calculus with sums of elementary tensors of fixed rank. *Numer. Math.* **2012**, *122*, 469–488.
- (34) Sorber, L.; Van Barel, M.; De Lathauwer, L. Optimization-Based Algorithms for Tensor Decompositions: Canonical Polyadic Decomposition, Decomposition in Rank- $(L_r, L_r, 1)$ Terms, and a New Generalization. *SIAM J. Optim.* **2013**, *23*, 695–720.
- (35) Navasca, C.; De Lathauwer, L.; Kindermann, S. Swamp Reducing Technique For Tensor Decomposition. 2008 16th European Signal Processing Conference. 2008; pp 1–5.
- (36) Whitten, J. L. Coulombic Potential Energy Integrals and Approximations. *J. Chem. Phys.* **1973**, *58*, 4496–4501.
- (37) Dunlap, B. I.; Connolly, J. W. D.; Sabin, J. R. On First-Row Diatomic Molecules and Local Density Models. *J. Chem. Phys.* **1979**, *71*, 4993.

- (38) Vahtras, O.; Almlöf, J.; Feyereisen, M. W. Integral approximations for LCAO-SCF calculations. *Chem. Phys. Lett.* **1993**, *213*, 514–518.
- (39) Jung, Y. Chemical Theory and Computation Special Feature: Auxiliary Basis Expansions for Large-Scale Electronic Structure Calculations. *Proc. Natl. Acad. Sci.* **2005**, *102*, 6692–6697.
- (40) Beebe, N. H. F.; Linderberg, J. Simplifications in the Generation and Transformation of Two-Electron Integrals in Molecular Calculations. *Int. J. Quantum Chem.* **1977**, *12*, 683–705.
- (41) Löwdin, P.-O. Studies in Perturbation Theory. IX. Connection between Various Approaches in the Recent Development—Evaluation of Upper Bounds to Energy Eigenvalues in Schrödinger’s Perturbation Theory. *J. Math. Phys.* **1965**, *6*, 1341–1353.
- (42) Löwdin, P.-O. Some properties of inner projections. *Int. J. Quantum Chem.* **2009**, *5*, 231–237.
- (43) Folkestad, S. D.; Kjøenstad, E. F.; Koch, H. An efficient algorithm for Cholesky decomposition of electron repulsion integrals. *J. Chem. Phys.* **2019**, *150*, 194112.
- (44) Lee, J.; Lin, L.; Head-Gordon, M. Systematically Improvable Tensor Hypercontraction: Interpolative Separable Density-Fitting for Molecules Applied to Exact Exchange, Second- and Third-Order Møller-Plesset Perturbation Theory. *J. Chem. Theory Comput.* **2020**, *16*, 243–263.
- (45) Hummel, F.; Tsatsoulis, T.; Grüneis, A. Low Rank Factorization of the Coulomb Integrals for Periodic Coupled Cluster Theory. *J. Chem. Phys.* **2017**, *146*, 124105.
- (46) Friesner, R. A. Solution of the Hartree–Fock equations by a pseudospectral method: Application to diatomic molecules. *J. Chem. Phys.* **1986**, *85*, 1462–1468.

- (47) Langlois, J.; Muller, R. P.; Coley, T. R.; Goddard, W. A.; Ringnalda, M. N.; Won, Y.; Friesner, R. A. Pseudospectral generalized valence-bond calculations: Application to methylene, ethylene, and silylene. *J. Chem. Phys.* **1990**, *92*, 7488–7497.
- (48) Ringnalda, M. N.; Belhadj, M.; Friesner, R. A. Pseudospectral Hartree–Fock Theory: Applications and Algorithmic Improvements. *J. Chem. Phys.* **1990**, *93*, 3397–3407.
- (49) Friesner, R. A. New Methods For Electronic Structure Calculations on Large Molecules. *Annu. Rev. Phys. Chem.* **1991**, *42*, 341–367.
- (50) Martinez, T. J.; Carter, E. A. Pseudospectral multireference single and double excitation configuration interaction. *J. Chem. Phys.* **1995**, *102*, 7564–7572.
- (51) Martinez, T. J.; Mehta, A.; Carter, E. A. Pseudospectral Full Configuration Interaction. *J. Chem. Phys.* **1992**, *97*, 1876–1880.
- (52) Martinez, T. J.; Carter, E. A. Pseudospectral Møller–Plesset perturbation theory through third order. *J. Chem. Phys.* **1994**, *100*, 3631–3638.
- (53) Ko, C.; Malick, D. K.; Braden, D. A.; Friesner, R. A.; Martínez, T. J. Pseudospectral time-dependent density functional theory. *J. Chem. Phys.* **2008**, *128*, 104103.
- (54) Martinez, T. J.; Carter, E. A. Pseudospectral double excitation configuration interaction. *J. Chem. Phys.* **1993**, *98*, 7081–7085.
- (55) Hohenstein, E. G.; Parrish, R. M.; Sherrill, C. D.; Martínez, T. J. Communication: Tensor Hypercontraction. III. Least-squares Tensor Hypercontraction for the Determination of Correlated Wavefunctions. *J. Chem. Phys.* **2012**, *137*, 221101.
- (56) Parrish, R. M.; Hohenstein, E. G.; Martínez, T. J.; Sherrill, C. D. Tensor Hypercontraction. II. Least-squares Renormalization. *J. Chem. Phys.* **2012**, *137*, 224106.

- (57) Hohenstein, E. G.; Kokkila, S. I. L.; Parrish, R. M.; Martinez, T. J. Quartic scaling second-order approximate coupled cluster singles and doubles via tensor hypercontraction: THC-CC2. *J. Chem. Phys.* **2013**, *138*, 124111.
- (58) Shenvi, N.; Van Aggelen, H.; Yang, Y.; Yang, W.; Schwerdtfeger, C.; Mazziotti, D. Low rank factorization of the Coulomb integrals for periodic coupled cluster theory. *J. Chem. Phys.* **2013**, *139*, 54110.
- (59) Schutski, R.; Zhao, J.; Henderson, T. M.; Scuseria, G. E. Tensor-structured coupled cluster theory. *J. Chem. Phys.* **2017**, *147*, 184113.
- (60) Parrish, R. M.; Zhao, Y.; Hohenstein, E. G.; Martinez, T. J. Rank reduced coupled cluster theory. I. Ground state energies and wavefunctions. *J. Chem. Phys.* **2019**, *150*, 164118.
- (61) Greengard, L.; Rokhlin, V. A Fast Algorithm for Particle Simulations. *J. Comput. Phys.* **1987**, *73*, 325–348.
- (62) Beylkin, G.; Cheruvu, V.; Perez, F. Fast Adaptive Algorithms in the Non-Standard Form for Multidimensional Problems. *Appl. Comput. Harmon. Anal.* **2008**, *24*, 354–377.
- (63) BTAS Library. 2021; <https://github.com/BTAS/BTAS>, Accessed: 2019-04-09.
- (64) Kroonenberg, P. M.; de Leeuw, J. Principal Component Analysis of Three-Mode Data by Means of Alternating Least Squares Algorithms. *Psychometrika* **1980**, *45*, 69–97.
- (65) Řezáč, J.; Riley, K. E.; Hobza, P. S66: A Well-Balanced Database of Benchmark Interaction Energies Relevant to Biomolecular Structures. *J. Chem. Theory Comput.* **2011**, *7*, 2427–2438.
- (66) Rezac J.; Jurecka P.; Riley K. E.; Cerny J.; Valdes H.; Pluhackova K.; Berka K.; Rezac T.; Pitonak M.; Vondrasek J.; Hobz, P. Quantum chemical benchmark energy and geom-

- etry database for molecular clusters and complex molecular systems (www.begdb.com): A users manual and examples. *Collect. Czechoslov. Chem. Commun.* **2008**, *73*, 1261–1270.
- (67) Jørgensen, P.; Simons, J. Ab Initio Analytical Molecular Gradients and Hessians. *J. Chem. Phys.* **1983**, *79*, 334–357.
- (68) Wales, D. J.; Hodges, M. P. Global minima of water clusters $(\text{H}_2\text{O})_n$, $n \leq 21$, described by an empirical potential. *Chem. Phys. Lett.* **1998**, *286*, 65–72.
- (69) Dunning, T. H. Gaussian basis sets for use in correlated molecular calculations. I. The atoms boron through neon and hydrogen. *J. Chem. Phys.* **1989**, *90*, 1007–1023.
- (70) Kendall, R. A.; Früchtl, H. A. The Impact of the Resolution of the Identity Approximate Integral Method on Modern Ab Initio Algorithm Development. *Theor. Chim. Acta* **1997**, *97*, 158–163.
- (71) Weigend, F.; Köhn, A.; Hättig, C. Efficient Use of the Correlation Consistent Basis Sets in Resolution of the Identity MP2 Calculations. *J. Chem. Phys.* **2002**, *116*, 3175.
- (72) Peterson, K. A.; Adler, T. B.; Werner, H.-J. Systematically Convergent Basis Sets for Explicitly Correlated Wavefunctions: The Atoms H, He, B-Ne, and Al-Ar. *J. Chem. Phys.* **2008**, *128*, 084102.
- (73) Espig, M.; Hackbusch, W. A Regularized Newton Method for the Efficient Approximation of Tensors Represented in the Canonical Tensor Format. *Numer. Math.* **2012**, *122*, 489–525.
- (74) Kazeev, V. A.; Tyrtysnikov, E. E. Structure of the Hessian Matrix and an Economical Implementation of Newton's Method in the Problem of Canonical Approximation of Tensors. *Comput. Math. and Math. Phys.* **2010**, *50*, 927–945.

- (75) Phan, A.-H.; Tichavský, P.; Cichocki, A. Low Complexity Damped Gauss–Newton Algorithms for CANDECOMP/PARAFAC. *SIAM J. Matrix Anal. & Appl.* **2013**, *34*, 126–147.